Electronic supplementary materials *Mendeleev Commun.*, 2022, **32**, 202–204

Decision problem with high residual electron density on the metal atom

Georgy K. Fukin, Anton V. Cherkasov and Roman V. Rumyantcev

Content

1. Calculation of the Terbium Atomic Invariom

The single point calculation of periodical 3D structure of $[Tb(Tpm)(Cl)_3]\cdot 2(MeCN)$ was performed within the PBE0 exchange-correlation functional[S1,S2] using CRYSTAL14.[S3] Atomic cores were described using modified all electron DZP basis set[S4–S6] (g functions has been omitted). The information from X-ray crystallography[S7] was used as geometry the atomic coordinates. The convergence of the PBE0 functional was optimized using the Broyden method.[S8] The shrinking factor of the reciprocal space was set to four, corresponding to 30 k points in the irreducible Brillouin zone at which the Hamiltonian matrix was diagonalized.

The VESTA (ver. 3.5.7) program[S9] was applied to generate 34821 unique Miller indices up to $s = 1.15$ Å^{-1} reciprocal resolution. The option XFAC of the CRYSTAL14 program was used to generate a set of theoretical structure factors from the electron density function, obtained by single-point calculation of the non-optimized experimental geometry. Based on the calculated structural amplitudes, using the MoPro program,[S10] the populations of the spherically symmetric valence shell (P_{val}) and the multipole parameters (P_{lm}) describing its deformation were obtained together with the corresponding expansion – contraction coefficients (k, k') for each atoms of $[Tb(Tpm)(Cl)_3]\cdot 2(MeCN)$ complex. The obtained values of P_{val}, P_{lm}, k and k' were used to multipole refinement by experimental reflections ($\sin\theta/\lambda = 1.1$ Å^{-1}) in real symmetry of complex for all atoms except terbium. In turn, the electronic parameters of Tb were left theoretical and not refined. The coordinates were refined for all atoms of the complex.

References

S1 J.P. Perdew, M. Ernzerhof, K. Burke, *J. Chem. Phys.*, 1996, **105**, 9982.

S2 C. Adamo, V. Barone, *J. Chem. Phys.*, 1999, **110**, 6158.

S3 R. Dovesi, R. Orlando, A. Erba, C.M. Zicovich-Wilson, B. Civalleri, S. Casassa, L. Maschio, M. Ferrabone, M. De La Pierre, Ph. D'Arco, Y. Noël, M. Causà, M. Rerat, B. Kirtman, *International Journal of Quantum Chemistry*, 2014, **114**, 1287.

S4 G.G. Camiletti, S.F. Machado, F.E. Jorge, *J. Comput. Chem.*, 2008, **29**, 2434.

S5 A. Canal Neto, E.P. Muniz, R. Centoducatte, F.E. Jorge, *J. Mol. Struct. THEOCHEM.*, 2005, **718**, 219.

S6 B.P. Pritchard, D. Altarawy, B. Didier, T.D. Gibson, Th.L. Windus, *J. Chem. Inf. Model.*, 2019, **59**, 4814.

S7 J. Long, D.M. Lyubov, T.V. Mahrova, A.V. Cherkasov, G.K. Fukin, Y. Guari, J. Larionova, A.A. Trifonov, *Dalton Trans.*, 2018, **47**, 5153.

S8 C. G. Broyden, *Math. Comput.*, 1965, **19**, 577.

S9 K. Momma and F. Izumi, *J. Appl. Crystallogr.*, 2011, **44**, 1272.

S10 C. Jelsch, B. Guillot, A. Lagoutte, C. Lecomte, *J. Appl. Crystallogr.*, 2005, **38**, 38.

Figure S1. Residual electron density (Q1=2.22 e·Å^{-3}; Q2=1.81 e·Å^{-3}; Q3=1.74 e·Å^{-3}) in $\mathbf{1_{iam}}$.

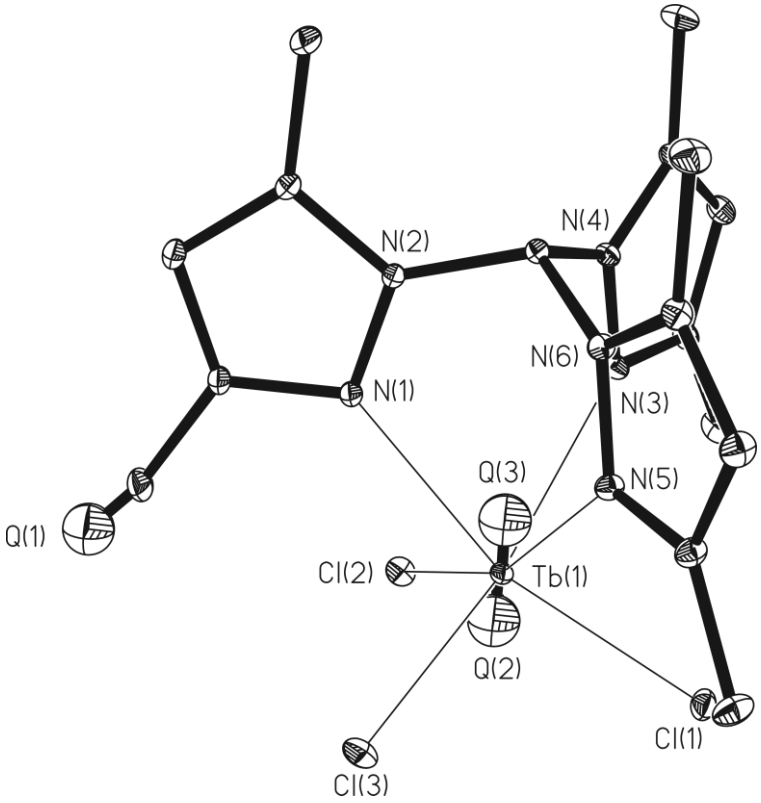

Figure S2. Isosurface of residual electron density (0.4 e·Å^{-3}) in unit cell of **1**$_{exp}$. Only one molecule of the complex is given for clarity. The maximum residual electron density is located at the C(5) atom (2.12 e·Å^{-3}).

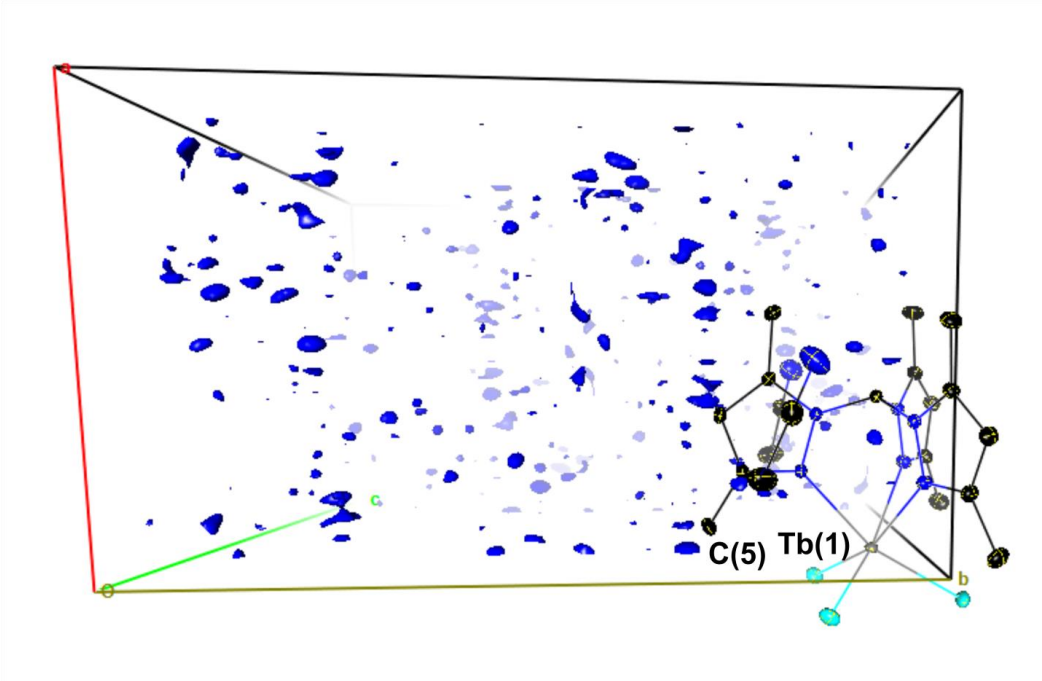

Figure S3. Isosurface of residual electron density (0.4 e·Å^{-3}) in unit cell of **1**$_{\mathbf{Tb\text{-}inv}}$. Only one molecule of the complex is given for clarity. The maximum residual electron density is located at the C(5) atom (2.14 e·Å^{-3}). The residual electron density near the terbium atom in **1**$_{\mathbf{Tb\text{-}inv}}$ is ~1.5 e Å^{-3}.

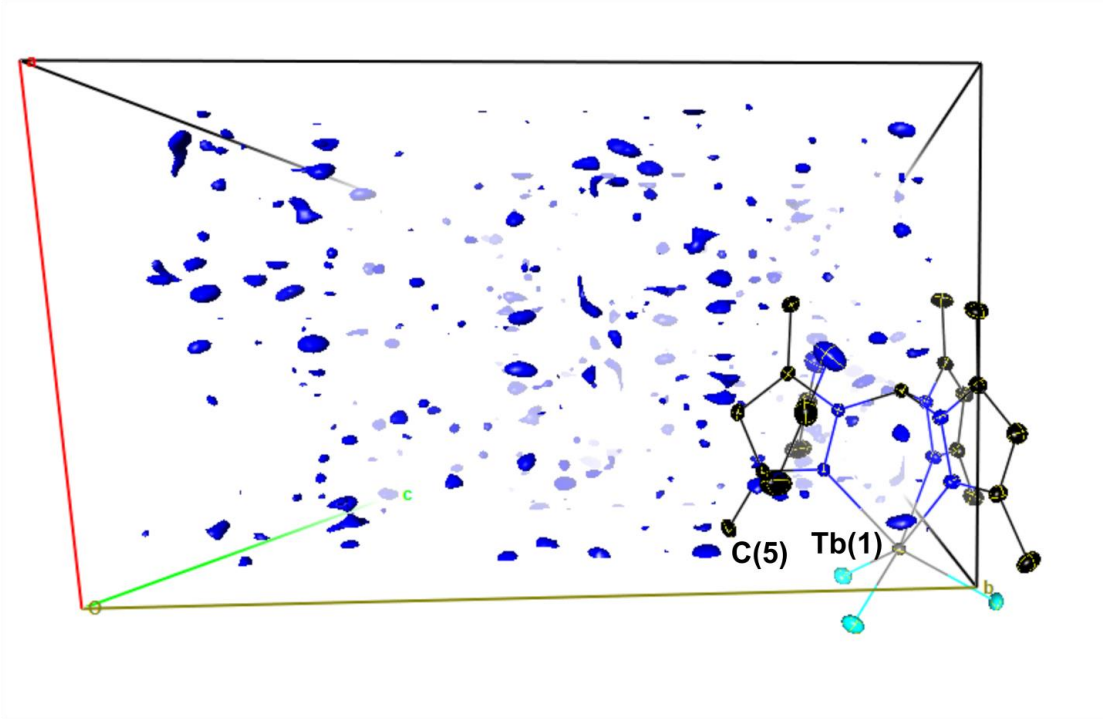

Figure S4. The deformation electron density (±0.05 e·Å^{-3}) in the plane of the Cl(1)Tb(1)Cl(2) fragment in **1**$_{exp}$.

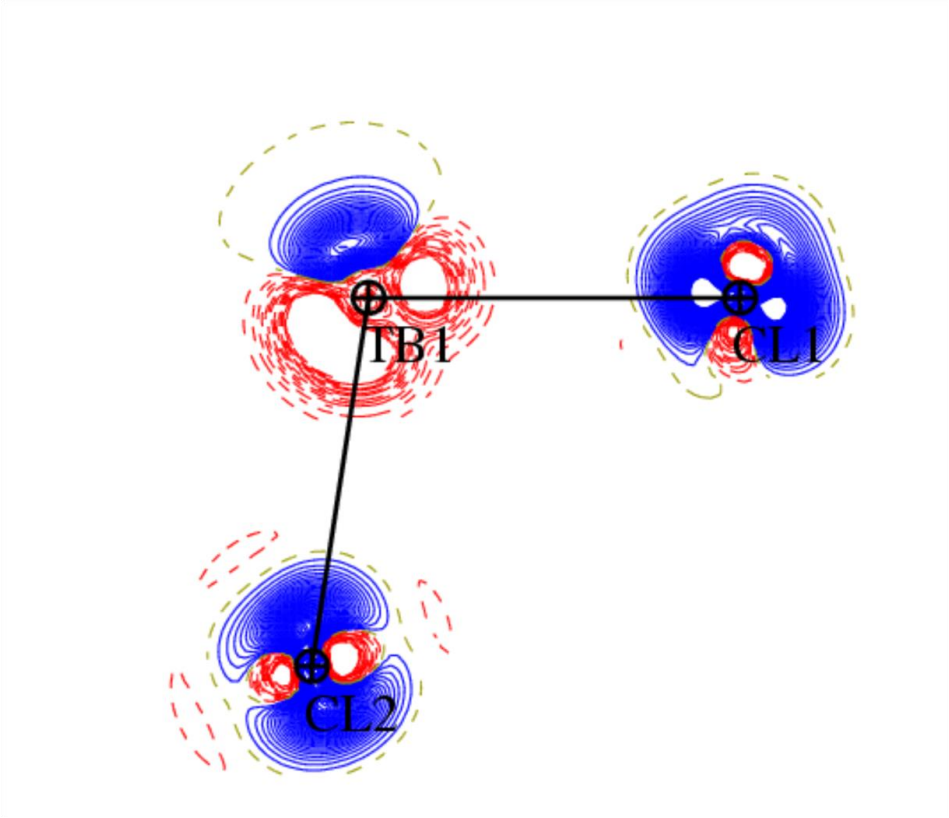

Figure S5. The deformation electron density (±0.05 e·Å^{-3}) in the plane of the N(3)Tb(1)Cl(2) fragment in **1**$_{exp}$.

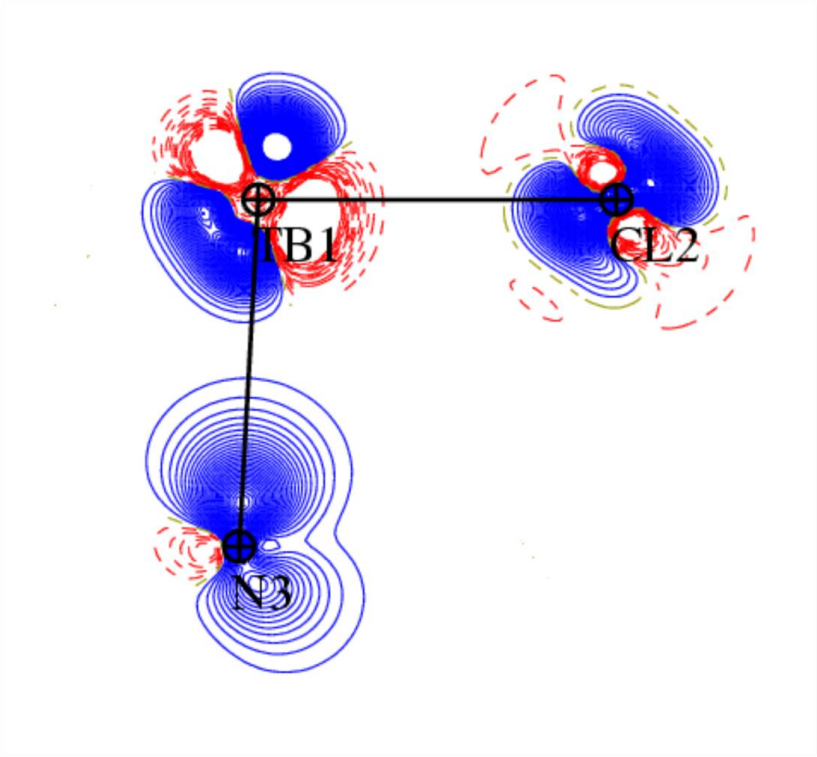

Figure S6. The deformation electron density (±0.05 e·Å^{-3}) in the plane of the N(5)Tb(1)N(3) fragment in **1**$_{exp}$.

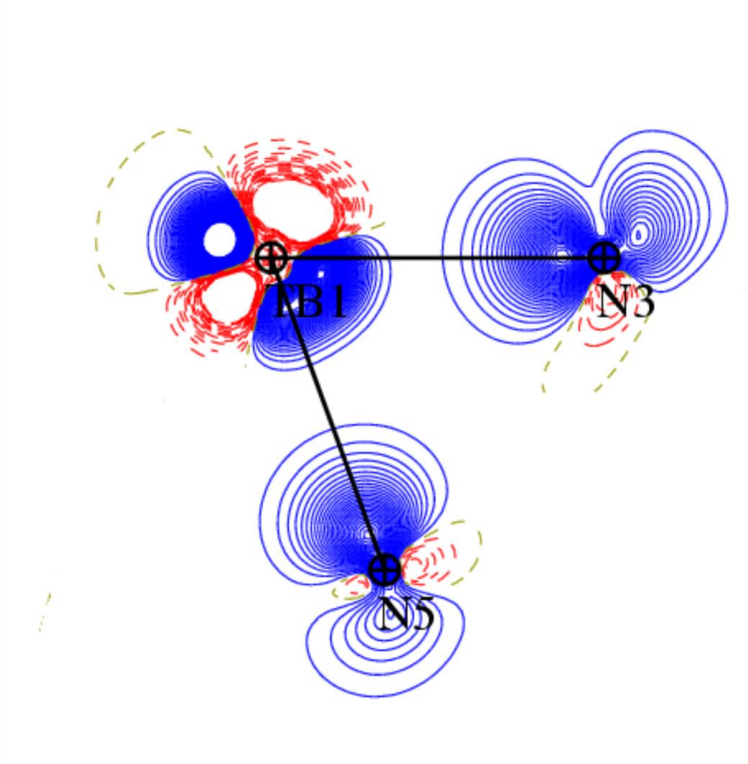

Figure S7. The deformation electron density (±0.05 e·Å^{-3}) in the plane of the Cl(1)Tb(1)Cl(2) fragment in **1**$_{\mathbf{Tb\text{-}inv.}}$

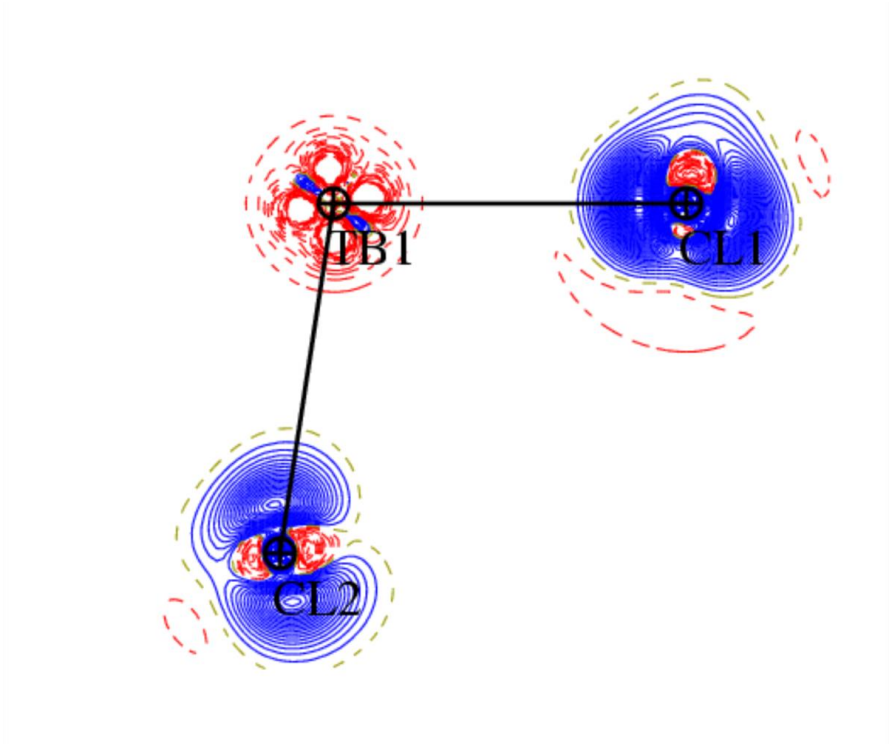

Figure S8. The deformation electron density (±0.05 e·Å^{-3}) in the plane of the Cl(2)Tb(1)N(3) fragment in **1**$_{\mathbf{Tb\text{-}inv.}}$

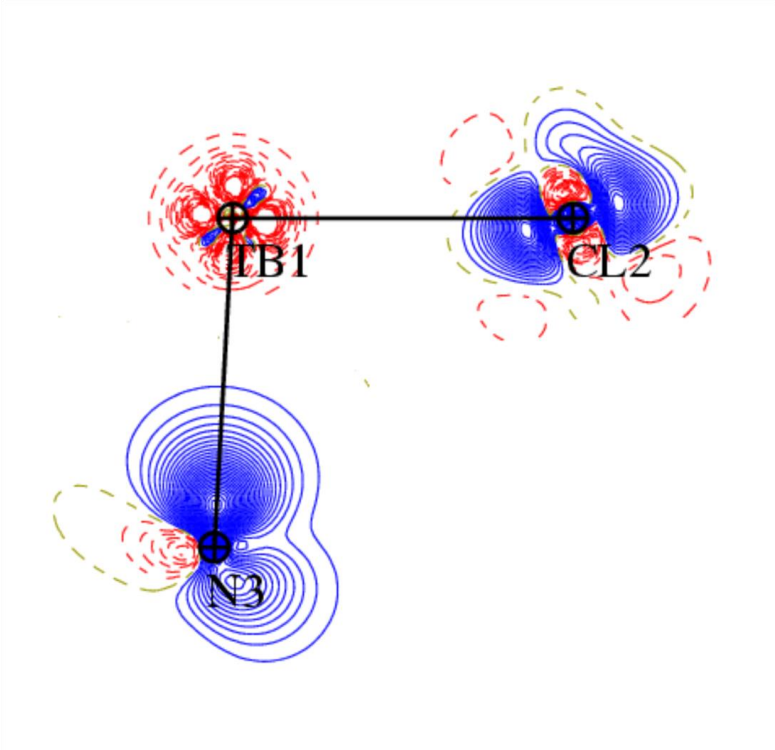

Figure S9. The deformation electron density (±0.05 e·Å^{-3}) in the plane of the N(3)Tb(1)N(5) fragment in **1**$_{\mathbf{Tb\text{-}inv.}}$

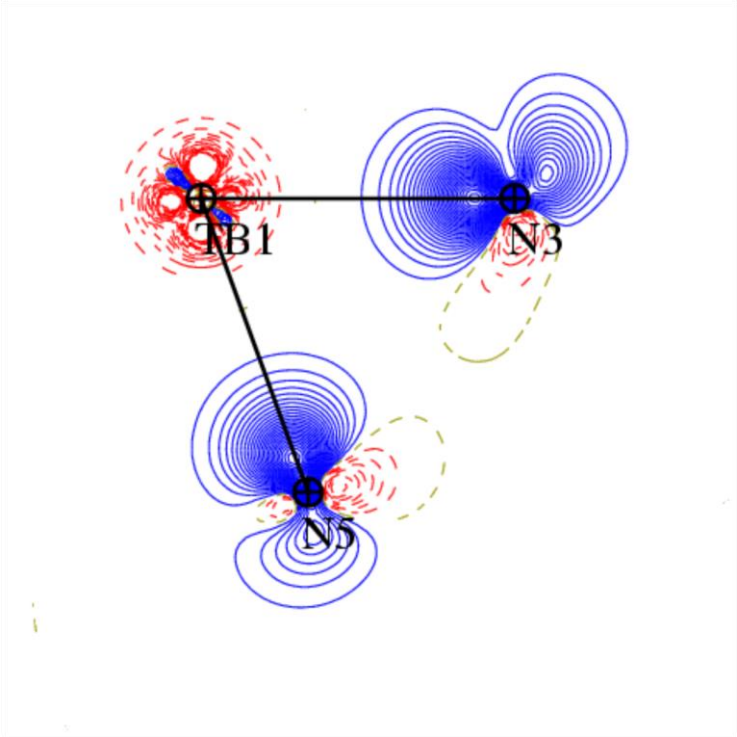

Figure S10. Experimental-theoretical molecular graph of complex $\mathbf{1}_{\mathbf{Tb\text{-}inv}}$.

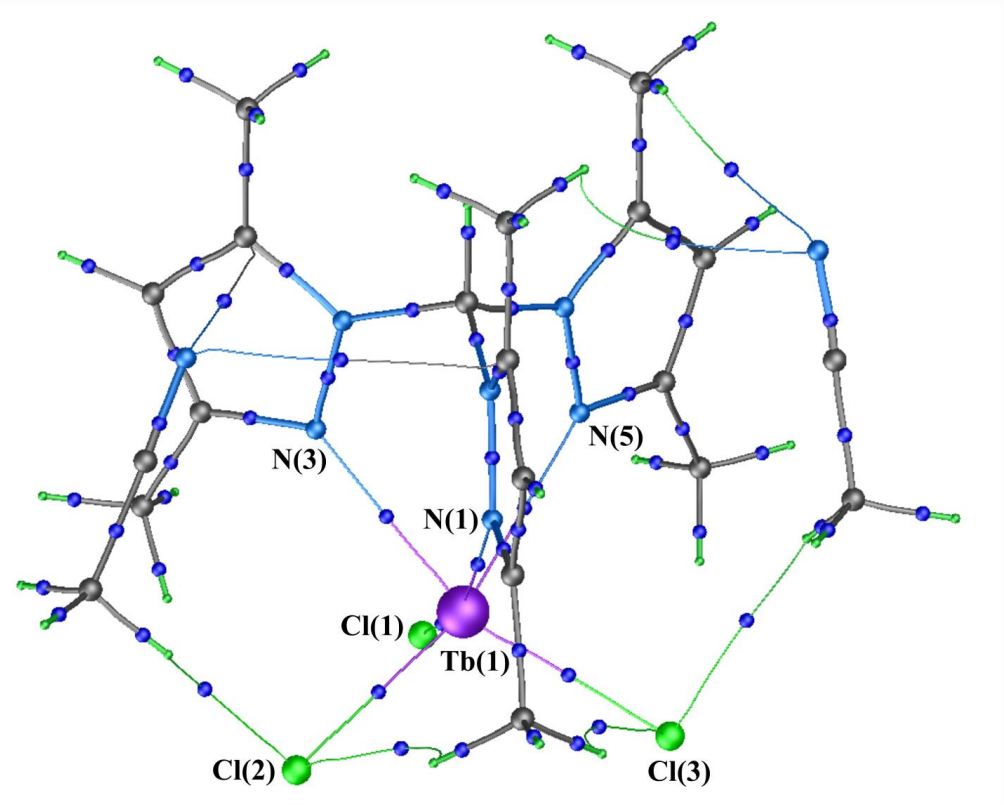

Figure S11. Fo/Fc vs resolution

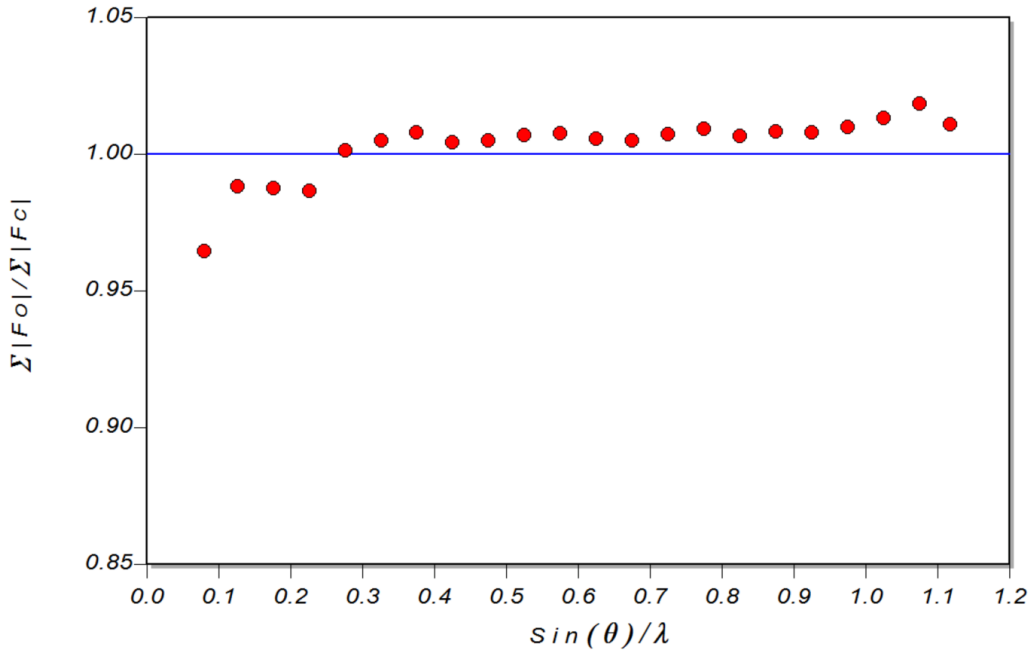

Figure S12. Normal probability

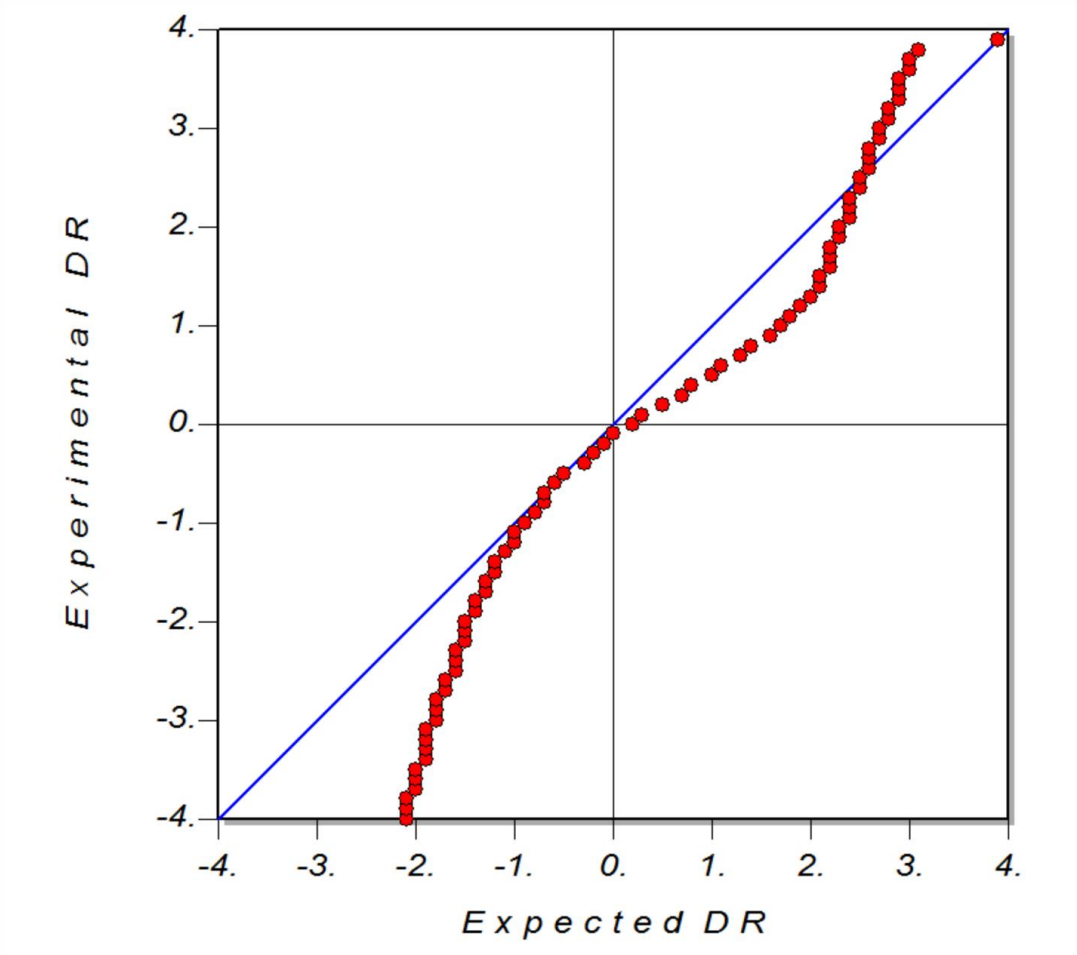

Figure S13. Fractal dimension vs residual density

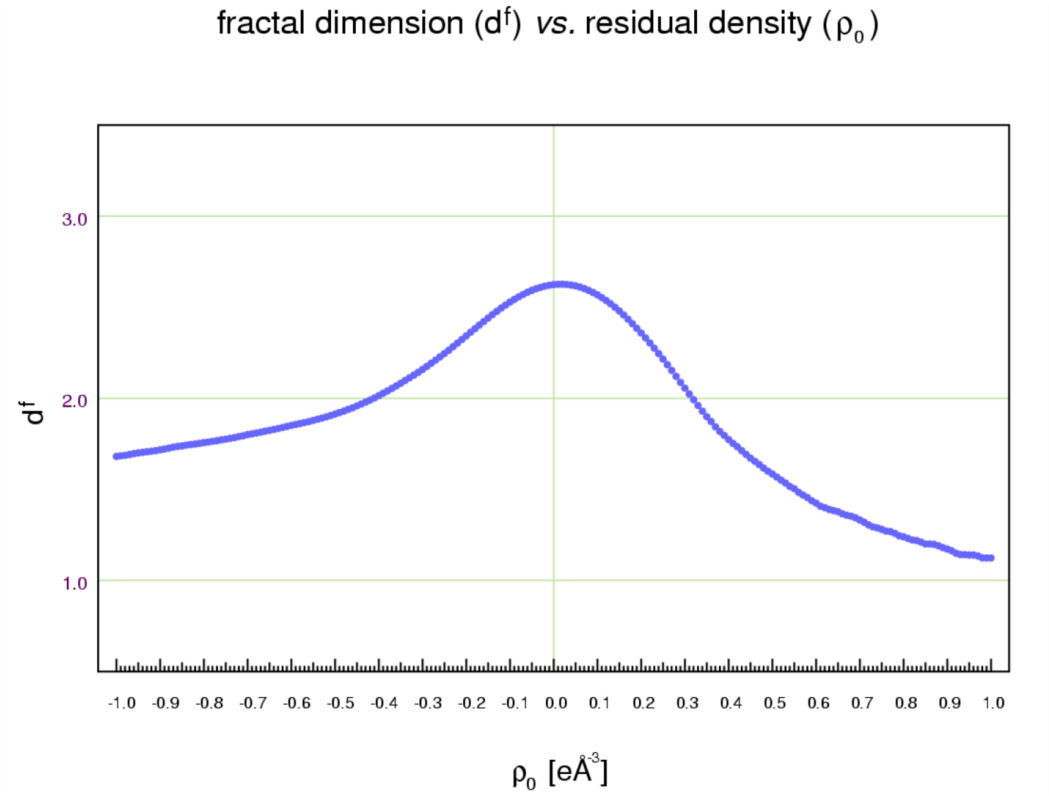

Table S1. Selected angles (deg) in the complex $\mathbf{1}_{exp}$.

Angle	Value (deg)	Angle	Value (deg)	Angle	Value (deg)
N(1)-TB1-N(3)	73.73(2)	N(1)-TB1-N(5)	74.636(19)	N(3)-TB1-N(5)	70.00(2)
Cl(1)-TB1-Cl(2)	98.723(8)	Cl(1)-TB1-Cl(3)	101.009(8)	Cl(2)-TB1-Cl(3)	102.531(8)
Cl(1)-TB1-N(1)	162.779(13)	Cl(2)-TB1-N(5)	160.399(14)	Cl(3)-TB1-N(3)	157.915(13)
Cl(1)-TB1-N(3)	91.701(15)	Cl(2)-TB1-N(1)	91.364(15)	Cl(3)-TB1-N(1)	90.280(15)
Cl(1)-TB1-N(5)	91.970(14)	Cl(2)-TB1-N(3)	93.176(14)	Cl(3)-TB1-N(5)	91.387(15)